ICIC Express Letters
Part B: Applications
Volume **14**, Number **11**, November **2023**

ICIC International ©2023 ISSN 2185-2766
pp. 1169–1177

LEADER-FOLLOWING FORMATION CONTROL OF VISUAL FIELD LIMITED UNICYCLE-TYPE MOBILE ROBOT WITH PRESCRIBED PERFORMANCE

Baoyu Wen and Jiangshuai Huang

School of Automation
Chongqing University
No. 174, Shazheng Street, Shapingba, Chongqing 400044, P. R. China
{ wenbaoyu; jshuang }@cqu.edu.cn

Received February 2023; accepted April 2023

Abstract. *In this paper, the transient performance for leader-following control of unicycle-type mobile robot with limited visual field is considered. Due to the limited detection range of sensors loaded on mobile robot, the field-of-view constraint is considered to ensure that mobile robot can always detect its leader. The prescribed performance bound (PPB) technique is introduced to ensure the transient and steady-state performance. In addition, the prescribed performance function used in this paper is different from the traditional one. Based on the fixed-time control design and Lyapunov analysis, leader-following formation tracking errors are shown to converge to a small neighborhood of zero in fixed settling time. An example is illustrated to show the effectiveness of the proposed control scheme.*
Keywords: Leader-following control, Prescribed performance, Field-of-view constraint

1. **Introduction.** Compared with other robots, wheeled mobile robots are more widely used because of their simple electrical structure, strong mobility, low energy loss and low hardware cost. For example, a large number of wheeled mobile robots have been used to carry goods autonomously. The unicycle-type mobile robot is a typical nonholonomic system. As a type of wheeled robot, its cost is greatly reduced on the premise of sacrificing only part of the maneuverability. Therefore, it is more widely used in various fields and there are many studies on it. In [1], the wheeled mobile robot model under nonholonomic constraints is constructed as a simple chain structure, and a trajectory tracking controller is designed through local linearization. In [2], a time-varying feedback tracking method is designed based on the backstepping method, which realizes the global trajectory tracking of the wheeled mobile robot with any initial error within the desired speed range. In [3], for a class of nonholonomic system, a tracking controller is designed and it allows global tracking of arbitrary reference trajectories. In [4], a trajectory tracking controller is designed at actuator level, which guarantees that the nonholonomic mobile robot tracks a given trajectory. Other related works of nonholonomic mobile robots include [5-9], but are not limited to these.

As one of the most attractive topics in the field of multi-agent systems, formation control has formed several typical control methods in many years of robot control research, including leader-following method [10, 11], virtual structure method [12, 13], behavior-based method [14, 15], etc. Of these methods, the leader-follower is not mathematically difficult to comprehend. In addition, it has good scalability, as the distance and angle required to maintain between a leader and a follower can be easily extended to the problem of formation control for multiple robots in a similar way. Therefore, the leader-follower

DOI: 10.24507/icicelb.14.11.1169

approach has been extensively applied to the formation control, and this method will be used in this paper.

From the perspective of practical application, the performance of the sensor is limited, which means that the detection distance and detection angle of the robot are limited [16, 17]. If the detection range of the robot is exceeded, the robots cannot communicate with each other. To solve this problem, the connectivity maintenance is considered in [18]. In addition, the transient performance control of the system is sometimes important in practical application. For a system, in addition to asymptotic convergence, it is usually desirable to have a fast convergence rate and a small tracking error at the initial stage of operation. By adding performance constraints to some state variables of formation system, then the design and analysis of the system are performed to evaluate its prescribed performance. In [19], for a class of multi-input multi-output feedback linearizable nonlinear systems, the attributes such as maximum overshoot, a lower bound of convergence speed and maximum allowable steady-state error are specified by introducing performance function. In [20], for a class of high-order nonlinear multi-agent systems, the prescribed transient and steady state performance is achieved by imposing the designer-specified performance functions. The barrier Lyapunov functions (BLF) have been proposed in the literature to solve the constraint problem, for example, the log-type symmetric or asymmetric BLF proposed in [21] and the tan-type BLFs proposed in [22-24]. For constrained and unconstrained systems, a new universal barrier function has been designed in [25, 26].

In the above part, the trajectory tracking, formation control methods, limited field of view and prescribed performance constraints of nonholonomic mobile robots are briefly summarized. After the above discussion, the following issues are discussed by us. The leader-following control method will be applied to realizing the formation of robots. At the same time, filed-of-view constraints are added to keep the visibility and avoid collision between each follower and its leader. Besides, time-varying constraint functions are used to address the prescribed transient and steady-state performance of the controlled system. Furthermore, the fixed-time control technique is incorporated into the formation control design. The contributions of this paper are formally summarized as follows.

- For the nonholonomic mobile robot model studied in this paper, it is considered to be an underactuated system. The original two-input-three-output system is transformed into a two-input-two-output system by merging the errors in the X and Y directions into the distance errors.
- In order to ensure that the follower can detect the leader when the sensor detection range is limited, the field-of-vision constraint is considered. In addition, the prescribed performance of the system is guaranteed by PPB technology.
- The fixed settling time of formation tracking errors that converge to a small neighborhood near the origin is obtained by using the fixed-time control technique.

The paper is organized as follows. In Section 2, some preliminaries and problem formulation are shown. Section 3 shows the procedures of designing a fixed-time formation controller. In Section 4, one simulation example is given to verify the effectiveness of our designed control strategies. Section 5 concludes this paper.

2. Problem Formulation and Preliminaries.

2.1. **Problem formulation.** The investigated NMR is a typical two-wheeled driven mobile robot as shown in Figure 1. In this paper, we consider a group of N two-wheeled mobile robots. The velocity of the each two driving wheels (v_{il} and v_{ir}) can result in linear velocity $v_i = (v_{ir} + v_{il})/2$. Angular velocity $\omega_i = \frac{r_i}{2}(\omega_{ir} - \omega_{il})/b_i$ with the half distance between two wheels being b_i and the radius of the wheel being r_i (for $i = 1, \ldots, N$). The positions of the robot i are denoted by (x_i, y_i) and the orientation is θ_i. Then, the kinematics model of each robot can be described by

$$\dot{\mathbf{x}}_i = \begin{bmatrix} \dot{x}_i \\ \dot{y}_i \\ \dot{\theta}_i \end{bmatrix} = \begin{bmatrix} v_i \cos\theta_i \\ v_i \sin\theta_i \\ \omega_i \end{bmatrix} \tag{1}$$

and $\mathbf{x}_i = [x_i, y_i, \theta_i]^T$ is the state variable.

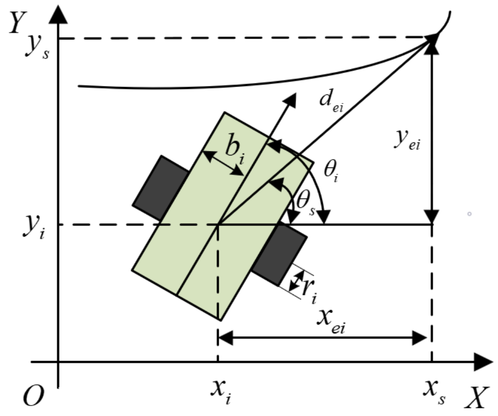

FIGURE 1. Geometric structure of leader-follower robots

A leader refers to the referenced model. As shown in Figure 1, a given reference trajectory which can be provided by another robot acts as a leader. In the leader-following structure, each robot acts according to local information. By maintaining the relative distance d_{ei} and relative bearing angle θ_{ei} between robots as defined below, a predetermined formation can be realized.

$$x_{ei} = x_s - x_i \quad y_{ei} = y_s - y_i \quad d_{ei} = \sqrt{x_{ei}^2 + y_{ei}^2} \tag{2}$$

$$\theta_{ei} = \theta_s - \theta_i \tag{3}$$

where x_s and y_s are the position of the leader in the X and Y directions, respectively. x_{ei} and y_{ei} represent the distance between robot i and the leader in the X and Y directions, respectively. $\theta_s = \arcsin \frac{y_{ei}}{d_{ei}}$ is the orientation of the leader.

Following from the above relations, the derivatives of d_{ei} and θ_{ei} are calculated as

$$\dot{d}_{ei} = -\cos(\theta_{ei})v + \left(\frac{x_{ei}}{d_{ei}}x'_d + \frac{y_{ei}}{d_{ei}}y'_d\right)\dot{s} \tag{4}$$

$$\dot{\theta}_{ei} = \omega + \frac{y_{ei}}{d_{ei}^2}\left(x'_d\dot{s} - v\cos(\theta)\right) - \frac{x_{ei}}{d_{ei}^2}\left(y'_d\dot{s} - v\sin(\theta)\right) \tag{5}$$

where $x'_d = \frac{\partial x_s}{\partial s}$, $y'_d = \frac{\partial y_s}{\partial s}$, s is the reference trajectory parameter.

1) Field-of-view constraints: The above defined $d_{ei}(t)$ and $\theta_{ei}(t)$ satisfy the following constraints:

$$\underline{d}_{ei} < d_{ei}(t) < \bar{d}_{ei}, \quad -\bar{\theta}_{ei} < \theta_{ei}(t) < \bar{\theta}_{ei} \quad \forall t \geq 0 \tag{6}$$

where $\bar{d}_{ei}$ represents the maximum detection range of the mobile robot, $\bar{\theta}_{ei}$ represents the maximum detection angle, and $\underline{d}_{ei}$ meeting $0 < \underline{d}_{ei} < \bar{d}_{ei}$ refers to the safe distance. It can be observed that through such constraints, ill-defined of systems (4) and (5) in $d_{ei} = 0$ and $\theta_{ei} = \frac{\pi}{2}$ can be avoided.

Define the formation tracking errors

$$z_{di} = d_{ei} - d_{di}, \quad z_{\theta i} = \theta_{ei} - \theta_{di} \tag{7}$$

where d_{di} and θ_{di} are the desired distance and angle, respectively. In this paper, they are considered as constants and meet conditions $\underline{d}_{ei} < d_{di} < \bar{d}_{ei}$ and $-\bar{\theta}_{ei} < \theta_{di} < \bar{\theta}_{ei}$.

2) Performance constraints: If $z_{di}(t)$ and $z_{\theta i}(t)$ satisfy the following inequalities:

$$\alpha_{1i}\eta_i(t) < z_{di}(t) < \beta_{1i}\eta_i(t), \quad -\alpha_{2i}\eta_i(t) < z_{\theta i}(t) < \beta_{2i}\eta_i(t) \tag{8}$$

with α_{1i}, β_{1i}, α_{2i} and β_{2i} being positive constants, the transient performances of $z_{di}(t)$ and $z_{\theta i}(t)$ can be guaranteed. Here, $\eta_i(t)$ is referred to as prescribed performance function (PPF).

The traditional PPF used in [18, 19, 24] is shown as follows:

$$\eta_i(t) = (\eta_{i0} - \eta_{i\infty})e^{-at} + \eta_{i\infty}$$

where $a > 0$, $\eta_{i0} > \eta_{i\infty} > 0$ are parameters to be selected. Clearly, $\eta_i(t) \leq \eta_{i0}$ and $\lim_{t\to\infty} \eta_i(t) = \eta_{i\infty}$. However, there is a limitation in traditional PPF. It is the final value $\eta_{i\infty}$ which is reached only when $t = +\infty$, which means that the user does not know the exact convergence time. To overcome these two drawbacks, the following PPF function [27] is introduced:

$$\begin{cases} \eta_i(0) = \eta_{i0} \\ \dot{\eta}_i(t) = -c_1(\eta_i(t) - \eta_{i\infty})^a - c_2(\eta_i(t) - \eta_{i\infty})^\gamma \end{cases} \tag{9}$$

where c_1, c_2, a and γ are positive constants, and $0 < a < 1$ and $\gamma > 1$.

If the selected α_{1i}, β_{1i}, α_{2i}, β_{2i}, η_{i0} and $\eta_{i\infty}$ satisfy the following inequalities

$$\alpha_{1i} \geq \frac{\underline{d}_{ei}}{\eta_{i\infty}} - d_{di} \quad \beta_{1i} \leq \frac{\bar{d}_{ei}}{\eta_{i0}} - d_{di} \quad \alpha_{2i} \leq \frac{\pi}{2\eta_{i0}} - \theta_{di} \quad \beta_{2i} \leq \frac{\pi}{2\eta_{i0}} - \theta_{di} \tag{10}$$

then, as long as Equation (8) is satisfied, (6) will always be true.

2.2. **Preliminaries.** In order to study the formation control of nonholonomic mobile robots, two assumptions and two lemmas are given here for subsequent analysis.

Assumption 2.1. *The robot is placed at the given position without violating the constraint (6) at the initial time* $t = 0$, *i.e.,* $\underline{d}_{ei} < d_{ei}(0) < \bar{d}_{ei}$ *and* $-\bar{\theta}_{ei} < \theta_{ei}(0) < \bar{\theta}_{ei}$.

Assumption 2.2. *Assume that the directed graph* $\bar{\mathcal{G}}$ *is connected and the leader is the root of the spanning tree.*

Lemma 2.1. *For* $p = 1 - \frac{1}{\lambda}$, $q = 1 + \frac{1}{\lambda}$, *where* $\lambda > 1$ *and* $x \geq 0$, *it can be known that the following inequality holds:*

$$-x^2 \leq -x^p - x^q + 1$$

Lemma 2.2. *If there exits a Lyapunov function* $W(x(t))$ *such that*

$$\dot{W}(x(t)) \leq -aW^p(x(t)) - bW^q(x(t)) + \sigma$$

where $a > 0$, $b > 0$, $0 < p < 1$, $q > 1$, $\sigma \in (0, +\infty)$, *then the system is practical fixed-time stable, and the convergence region of the system is*

$$\left\{ \lim_{t\to T} |W(x(t)) \leq \min\left\{ a^{-\frac{1}{p}} \left(\frac{\sigma}{1-\varphi}\right)^{\frac{1}{p}}, b^{-\frac{1}{q}} \left(\frac{\sigma}{1-\varphi}\right)^{\frac{1}{q}} \right\} \right\}$$

where φ *is a constant that satisfies* $0 < \varphi < 1$. *The settling time function* T *can be estimated by*

$$T \leq T_{\max} := \frac{1}{a\varphi(1-p)} + \frac{1}{b\varphi(q-1)}$$

3. **Design of Fixed-Time Formation Controller.** Define the following error variables

$$\rho = \frac{z_{di}}{\eta_i}, \quad \chi = \frac{z_{\theta i}}{\eta_i} \tag{11}$$

Let

$$\delta = \frac{\bar{\rho}\underline{\rho}\rho(t)}{(\bar{\rho} - \rho(t))\left(\rho(t) + \underline{\rho}\right)}, \quad \zeta = \frac{\bar{\chi}\underline{\chi}\chi(t)}{(\bar{\chi} - \chi(t))\left(\chi(t) + \underline{\chi}\right)} \tag{12}$$

Choose the following Lyapunov candidate function

$$V = \frac{1}{2}\delta^2 + \frac{1}{2}\zeta^2 \tag{13}$$

Differentiating (13) along (11) and systems (4), (5) yields

$$\begin{aligned}\dot{V} = {} & f_\delta \left[\frac{1}{\eta_i}\left(-v\cos(\theta_{ei}) + \left(\frac{x_{ei}}{d_{ei}}{x'}_d + \frac{y_{ei}}{d_{ei}}{y'}_d\right)\dot{s}\right) - \frac{d_{ei}\dot{\eta}_i}{\eta_i^2}\right] \\ & + f_\zeta \left[\frac{1}{\eta_i}\left(\omega + \frac{y_{ei}}{d_{ei}^2}\left({x'}_d\dot{s} - v\cos(\theta)\right) - \frac{x_{ei}}{d_{ei}^2}\left({y'}_d\dot{s} - v\sin(\theta)\right)\right) - \frac{\theta_{ei}\dot{\eta}_i}{\eta_i^2}\right]\end{aligned} \tag{14}$$

where $f_\delta = \frac{\bar{\rho}^2\underline{\rho}^2\left(\rho^2+\bar{\rho}\underline{\rho}\right)\rho}{(\bar{\rho}-\rho)^3\left(\rho+\underline{\rho}\right)^3}$, $f_\zeta = \frac{\bar{\chi}^2\underline{\chi}^2\left(\chi^2+\bar{\chi}\underline{\chi}\right)\chi}{(\bar{\chi}-\chi)^3\left(\chi+\underline{\chi}\right)^3}$.

Then, design the following control laws

$$v = \frac{k_1\eta_i\bar{\rho}^2\underline{\rho}^2}{\cos(\theta_{ei})(\bar{\rho}-\rho)\left(\rho+\underline{\rho}\right)}\rho + \frac{1}{\cos(\theta_{ei})}\left[\left(\frac{x_{ei}}{d_{ei}}{x'}_d + \frac{y_{ei}}{d_{ei}}{y'}_d\right)\dot{s} - \frac{d_{ei}\dot{\eta}_i}{\eta_i}\right] \tag{15}$$

$$\omega = -\frac{k_2\eta_i\bar{\chi}^2\underline{\chi}^2}{(\bar{\chi}-\chi)\left(\chi+\underline{\chi}\right)}\chi - \frac{y_{ei}}{d_{ei}^2}\left({x'}_d\dot{s} - v\cos(\theta)\right) + \frac{x_{ei}}{d_{ei}^2}\left({y'}_d\dot{s} - v\sin(\theta)\right) + \frac{\theta_{ei}\dot{\eta}_i}{\eta_i} \tag{16}$$

Hence, the derivative of V can be rewritten as

$$\dot{V} = -\frac{k_1\bar{\rho}^2\underline{\rho}^2 f_\delta}{(\bar{\rho}-\rho)\left(\rho+\underline{\rho}\right)}\rho - \frac{k_2\bar{\chi}^2\underline{\chi}^2 f_\zeta}{(\bar{\chi}-\chi)\left(\chi+\underline{\chi}\right)}\chi \tag{17}$$

Following from the above relations, inequalities $-\frac{k_1\bar{\rho}^2\underline{\rho}^2 f_\delta}{(\bar{\rho}-\rho)\left(\rho+\underline{\rho}\right)}\rho \le -k_1\left[\frac{\bar{\rho}\underline{\rho}\rho}{(\bar{\rho}-\rho)\left(\rho+\underline{\rho}\right)}\right]^4$ and $-\frac{k_2\bar{\chi}^2\underline{\chi}^2 f_\zeta}{(\bar{\chi}-\chi)\left(\chi+\underline{\chi}\right)}\chi \le -k_2\left[\frac{\bar{\chi}\underline{\chi}\chi}{(\bar{\chi}-\chi)\left(\chi+\underline{\chi}\right)}\right]^4$ hold.

Hence, we can get

$$\dot{V} \le -k_1\left[\frac{\bar{\rho}\underline{\rho}\rho}{(\bar{\rho}-\rho)\left(\rho+\underline{\rho}\right)}\right]^4 - k_2\left[\frac{\bar{\chi}\underline{\chi}\chi}{(\bar{\chi}-\chi)\left(\chi+\underline{\chi}\right)}\right]^4 \tag{18}$$

By applying Lemma 2.1, we obtain

$$\begin{aligned}\dot{V} \le & -k_1\left[\frac{\bar{\rho}\underline{\rho}\rho}{(\bar{\rho}-\rho)(\rho+\underline{\rho})}\right]^{2p} - k_1\left[\frac{\bar{\rho}\underline{\rho}\rho}{(\bar{\rho}-\rho)(\rho+\underline{\rho})}\right]^{2q} + k_1 \\ & - k_2\left[\frac{\bar{\chi}\underline{\chi}\chi}{(\bar{\chi}-\chi)\left(\chi+\underline{\chi}\right)}\right]^{2p} - k_2\left[\frac{\bar{\chi}\underline{\chi}\chi}{(\bar{\chi}-\chi)\left(\chi+\underline{\chi}\right)}\right]^{2q} + k_2\end{aligned} \tag{19}$$

From (19), we can get

$$\dot{V} \le -\alpha V^p - \beta V^q + C \tag{20}$$

where $\alpha = \min\{2^p k_1, 2^p k_2\}$, $\beta = \min\{2k_1, 2k_2\}$, $C = k_1 + k_2$.

Theorem 3.1. *For the system (1) under Assumption 2.1 and the control laws given in (15) and (16), if p and q are chosen as Lemma 2.1, then we can draw the following conclusions.*

1) Using the performance function $\eta_i(t)$ shown in (9), the tracking errors $z_{di}(t)$ and $z_{\theta i}(t)$ will converge to the sets Ω_d and Ω_θ defined below, respectively.

$$\Omega_d = \left\{z_{di}(t)|\underline{\Gamma}_d\eta_i(t) \le z_{di}(t) \le \bar{\Gamma}_d\eta_i(t)\right\}, \quad \Omega_\theta = \left\{z_{\theta i}(t)|\underline{\Gamma}_\theta\eta_i(t) \le z_{\theta i}(t) \le \bar{\Gamma}_\theta\eta_i(t)\right\} \tag{21}$$

where $\underline{\Gamma}_d$, $\bar{\Gamma}_d$, $\underline{\Gamma}_\theta$ *and* $\bar{\Gamma}_\theta$ *will be designed later.* α *and* β *are given in (20), and constant* $\varpi \in (0,1)$. *The range of* Ω_d *and* Ω_θ *can be adjusted by selecting different design parameters. And the fixed time* T *is given in the following:*

$$T \le T_{\max} := \frac{1}{\alpha\varpi(1-p)} + \frac{1}{\beta\varpi(q-1)} \tag{22}$$

2) Both constraints shown in (6) and (8) can be guaranteed.
3) All signals in the closed-loop system are bounded.

Proof: 1) From Lemma 2.2, we can get when $t \to T$, $V \le \min\left\{\alpha^{-\frac{1}{p}}\left(\frac{C}{1-\varpi}\right)^{\frac{1}{p}}, \beta^{-\frac{1}{q}}\left(\frac{C}{1-\varpi}\right)^{\frac{1}{q}}\right\}$. According to the expression of V, one can get the inequality $\frac{1}{2}\delta^2 + \frac{1}{2}\zeta^2 \le \min\left\{\alpha^{-\frac{1}{p}}\left(\frac{C}{1-\varpi}\right)^{\frac{1}{p}}, \beta^{-\frac{1}{q}}\left(\frac{C}{1-\varpi}\right)^{\frac{1}{q}}\right\}$. Hence, the following inequalities

$$|\delta| \le \xi, \quad |\zeta| \le \xi \tag{23}$$

hold, where $\xi = \min\left\{\sqrt{2\alpha^{-\frac{1}{p}}\left(\frac{C}{1-\varpi}\right)^{\frac{1}{p}}}, \sqrt{2\beta^{-\frac{1}{q}}\left(\frac{C}{1-\varpi}\right)^{\frac{1}{q}}}\right\}$. As a result, we have

$$\left|\frac{\bar{\rho}\underline{\rho}\rho(t)}{(\bar{\rho}-\rho(t))\left(\rho(t)+\underline{\rho}\right)}\right| \le \xi, \quad \left|\frac{\bar{\chi}\underline{\chi}\chi(t)}{(\bar{\chi}-\chi(t))\left(\chi(t)+\underline{\chi}\right)}\right| \le \xi \tag{24}$$

By solving (24), we obtain

$$\underline{\Gamma}_d \le \rho(t) \le \bar{\Gamma}_d, \quad \underline{\Gamma}_\theta \le \chi(t) \le \bar{\Gamma}_\theta \tag{25}$$

where

$$\begin{aligned}
\underline{\Gamma}_d &= \frac{\xi\left(\bar{\rho}-\underline{\rho}\right) + \bar{\rho}\underline{\rho} - \sqrt{\left(\xi\bar{\rho}+\bar{\rho}\underline{\rho}-\xi\underline{\rho}\right)^2 + 4\xi^2\bar{\rho}\underline{\rho}}}{2\xi}, \\
\underline{\Gamma}_\theta &= \frac{\xi\left(\bar{\chi}-\underline{\chi}\right) + \bar{\chi}\underline{\chi} - \sqrt{\left(\xi\bar{\chi}+\bar{\chi}\underline{\chi}-\xi\underline{\chi}\right)^2 + 4\xi^2\bar{\chi}\underline{\chi}}}{2\xi}, \\
\bar{\Gamma}_d &= \frac{\xi\left(\bar{\rho}-\underline{\rho}\right) - \bar{\rho}\underline{\rho} + \sqrt{\left(\bar{\rho}\underline{\rho}-\xi\bar{\rho}+\xi\underline{\rho}\right)^2 + 4\xi^2\bar{\rho}\underline{\rho}}}{2\xi}, \\
\bar{\Gamma}_\theta &= \frac{\xi\left(\bar{\chi}-\underline{\chi}\right) - \bar{\chi}\underline{\chi} + \sqrt{\left(-\xi\bar{\chi}+\bar{\chi}\underline{\chi}+\xi\underline{\chi}\right)^2 + 4\xi^2\bar{\chi}\underline{\chi}}}{2\xi}
\end{aligned}$$

Combining (11) and (25), one can get that $z_{di}(t)$ and $z_{\theta i}(t)$ converge to Ω_d and Ω_θ in fixed time, respectively. And from Lemma 2.2, we can obtain the upper bound on the convergence time is $T_{\max} = \frac{1}{\alpha\varpi(1-p)} + \frac{1}{\beta\varpi(q-1)}$.

2) Here, parameters α_{1i}, β_{1i}, α_{2i} and β_{2i} are designed as $\alpha_{1i} \ge \max\left\{\underline{\Gamma}_d - d_{di}, \frac{d_{ei}}{\eta_{i\infty}} - d_{di}\right\}$, $\alpha_{2i} \le \min\left\{|\underline{\Gamma}_\theta| - d_{di}, \frac{\pi}{2\eta_{i0}} - d_{di}\right\}$, $\beta_{1i} \le \min\left\{\bar{\Gamma}_d - d_{\theta i}, \frac{\bar{d}_{ei}}{\eta_{i0}} - d_{\theta i}\right\}$, $\beta_{2i} \le \min\left\{\bar{\Gamma}_\theta - d_{\theta i}, \frac{\pi}{2\eta_{i0}} - d_{\theta i}\right\}$. Therefore, we can easily know the constraints on $d_{ei}(t)$ and $\theta_{ei}(t)$ are guaranteed.

3) From (20), we can get

$$\dot{V} \le -\alpha V^p - \beta V^q + C \le -2\sqrt{\alpha\beta}V + C \tag{26}$$

Integrate the above formula and get

$$V(t) \le \left(V(0) - \frac{C}{2\sqrt{\alpha\beta}}\right)\exp\left(-2\sqrt{\alpha\beta}t\right) + \frac{C}{2\sqrt{\alpha\beta}} \tag{27}$$

We can know V is ultimately bounded by $\frac{C}{2\sqrt{\alpha\beta}}$. This indicates that $|\delta|$ and $|\zeta|$ are bounded by $\sqrt{\frac{C}{\sqrt{\alpha\beta}}}$. Hence, one can know that all signals in the closed-loop system are bounded.

4. Simulation Results and Analysis. The formation tracking control problem for four identical mobile robots modeled by (1) is considered in this part. The system parameters are chosen as $b_i = 0.75$, $r_i = 0.15$. The reference trajectories are specified as $[s, 10\sin(0.1s)]$. The initial states are set as $x_1(0) = 0.2$, $y_1(0) = 9$, $x_2(0) = 10.5$, $y_2(0) = -0.2$, $x_3(0) = 0.2$, $y_3(0) = -9.3$, $x_4(0) = -9.8$, $y_4(0) = -0.3$. The simulation results are shown in Figures 2 and 3. From Figure 2, it can be seen that all the robots can track the reference trajectory effectively. Figure 3 shows that the tracking errors of robot 1 are constrained. Due to the length limitation of the paper, the tracking errors of other robots will not be shown here.

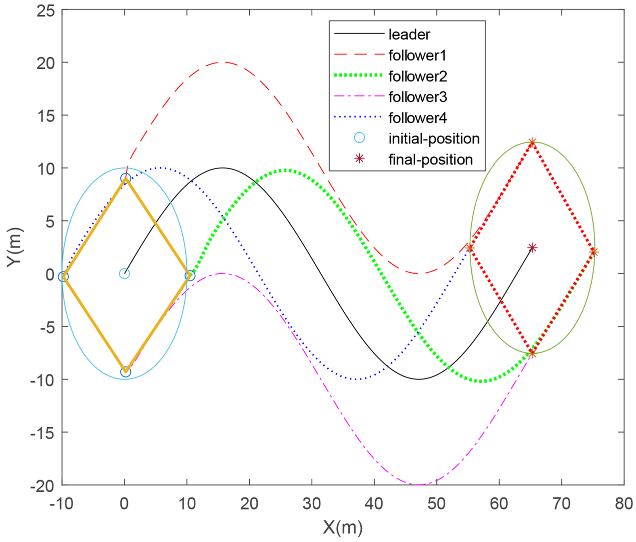

FIGURE 2. Robot position in (X, Y) plane

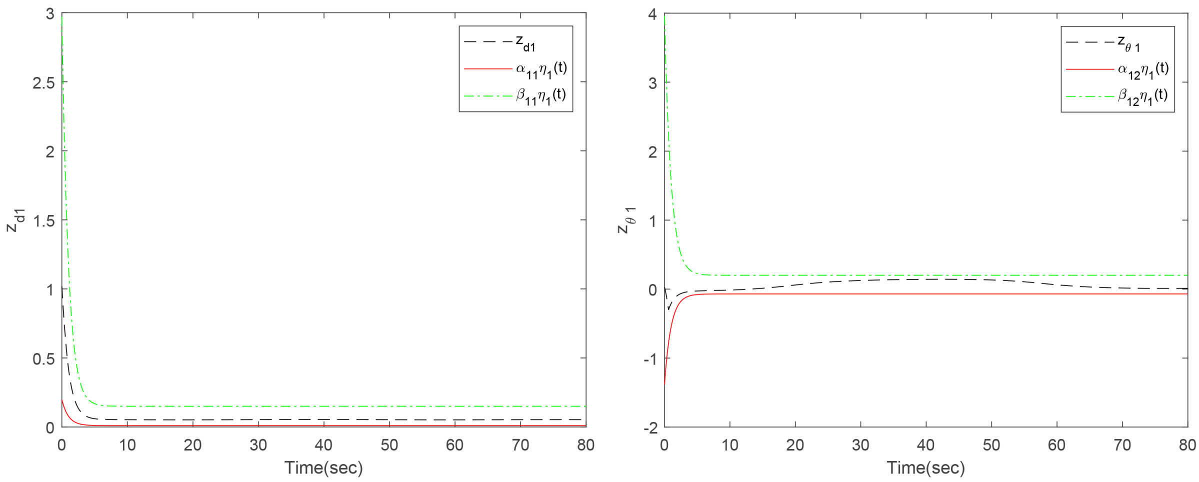

FIGURE 3. Tracking errors z_{d1} and $z_{\theta 1}$ of robot 1

5. Conclusion. The transient performance for leader-following control of unicycle-type mobile robots with limited visual field is investigated in this paper. The prescribed performance of formation tracking errors is guaranteed by applying PPB technique. And the performance function used in this paper is different from the traditional one. Besides, the fixed-time control is applied to showing the formation tracking errors converge to a small neighborhood of zero in fixed settling time. Finally, simulation results show the effectiveness of the proposed control scheme.

REFERENCES

[1] G. Walsh, D. Tilbury, S. Sastry et al., Stabilization of trajectories for systems with nonholonomic constraints, *IEEE Transactions on Automatic Control*, vol.39, no.1, pp.216-222, 1994.

[2] Z. P. Jiangdagger and H. Nijmeijer, Tracking control of mobile robots: A case study in backstepping, *Automatica*, vol.33, no.7, pp.1393-1399, 1997.

[3] M. Mauder, Robust tracking control of nonholonomic dynamic systems with application to the bi-steerable mobile robot, *Automatica*, vol.44, no.10, pp.2588-2592, 2008.

[4] J. Fu, F. Tian, T. Chai et al., Motion tracking control design for a class of nonholonomic mobile robot systems, *IEEE Transactions on Systems, Man, and Cybernetics: Systems*, vol.50, no.6, pp.2150-2156, 2018.

[5] P. Morin and C. Samson, Control of nonholonomic systems based on transverse function approach, *IEEE Transactions on Robotics*, vol.25, no.5, pp.1058-1073, 2009.

[6] T. C. Lee and Z. P. Jiang, Uniform asymtotic stability of nonlinear switched systems with an application to mobile robots, *IEEE Transactions on Automatic Control*, vol.53, no.5, pp.1235-1252, 2008.

[7] D. Tsankova, V. Georgieva and F. Zezulka, Immune network control for stigmergy based foraging behaviour of autonomous mobile robots, *International Journal of Adaptive Control and Signal Processing*, vol.21, nos.2-3, pp.256-286, 2007.

[8] A. Y. Alanis, M. Lopez-Franco and N. Arana-Daniel, Discrete-time neural control for electrically driven nonholonomic mobile robots, *International Journal of Adaptive Control and Signal Processing*, vol.26, no.7, pp.630-644, 2012.

[9] F. Yang, C. Wang and G. Jing, Adaptive tracking control for dynamic nonholonomic mobile robots with uncalibrated visual parameter, *International Journal of Adaptive Control and Signal Processing*, vol.27, no.8, pp.688-700, 2013.

[10] X. Liang, Y. H. Liu, H. Wang et al., Leader-following formation tracking control of mobile robots without direct position measurements, *IEEE Transactions on Automatic Control*, vol.61, no.12, pp.4131-4137, 2016.

[11] L. Consolini, F. Morbidi, D. Prattichizzo et al., Leader-follower formation control of nonholonomic mobile robots with input constraints, *Automatica*, vol.44, no.5, pp.1343-1349, 2008.

[12] A. Sadowska, T. Van Den Broek, H. Huijberts et al., A virtual structure approach to formation control of unicycle mobile robots using mutual coupling, *International Journal of Control*, vol.84, no.11, pp.1886-1902, 2011.

[13] Q. Zhang, L. Lapierre and X. Xiang, Distributed control of coordinated path tracking for networked nonholonomic mobile vehicles, *IEEE Transactions on Industrial Informatics*, vol.9, no.1, pp.472-484, 2013.

[14] J. R. T. Lawton, R. W. Beard and B. J. Young, A decentralized approach to formation maneuvers, *IEEE Transactions on Robotics and Automation*, vol.19, no.6, pp.933-941, 2003.

[15] F. Arrichiello, S. Chiaverini, G. Indiveri et al., The null-space based behavioral control for nonholonomic mobile robots with actuators velocity saturation, *International Journal of Robotics Research*, vol.29, no.10, pp.1317-1337, 2010.

[16] D. Panagou and V. Kumar, Cooperative visibility maintenance for leader-follower formations in obstacle environments, *IEEE Transactions on Robotics*, vol.30, no.4, pp.831-844, 2014.

[17] I. M. Delimpaltadakis, C. P. Bechlioulis and K. J. Kyriakopoulos, Decentralized platooning with obstacle avoidance for car-like vehicles with limited sensing, *IEEE Robotics and Automation Letters*, vol.3, no.2, pp.835-840, 2018.

[18] S. L. Dai, S. He, Y. Ma et al., Distributed cooperative learning control of uncertain multiagent systems with prescribed performance and preserved connectivity, *IEEE Transactions on Neural Networks and Learning Systems*, vol.32, no.7, pp.3217-3229, 2021.

[19] C. P. Bechlioulis and G. A. Rovithakis, Robust adaptive control of feedback linearizable MIMO nonlinear systems with prescribed performance, *IEEE Transactions on Automatic Control*, vol.53, no.9, pp.2090-2099, 2008.

[20] C. P. Bechlioulis and G. A. Rovithakis, Decentralized robust synchronization of unknown high order nonlinear multi-agent systems with prescribed transient and steady state performance, *IEEE Transactions on Automatic Control*, vol.62, no.1, pp.123-134, 2017.

[21] K. P. Tee, S. S. Ge and E. H. Tay, Barrier Lyapunov functions for the control of output-constrained nonlinear systems, *Automatica*, vol.45, no.4, pp.918-927, 2009.
[22] X. Jin and J. X. Xu, Iterative learning control for output-constrained systems with both parametric and nonparametric uncertainties, *Automatica*, vol.49, no.8, pp.2508-2516, 2013.
[23] X. Jin, Fault tolerant finite-time leader-follower formation control for autonomous surface vessels with LOS range and angle constraints, *Automatica*, vol.68, no.6, pp.228-236, 2016.
[24] S. L. Dai, S. He, X. Chen et al., Adaptive leader-follower formation control of nonholonomic mobile robots with prescribed transient and steady-state performance, *IEEE Transactions on Industrial Informatics*, vol.16, no.6, pp.3662-3671, 2020.
[25] X. Jin, Adaptive fixed-time control for MIMO nonlinear systems with asymmetric output constraints using universal barrier functions, *IEEE Transactions on Automatic Control*, vol.64, no.7, pp.3046-3053, 2019.
[26] K. Zhao, Y. Song and Z. Zhang, Tracking control of MIMO nonlinear systems under full state constraints: A single-parameter adaptation approach free from feasibility conditions, *Automatica*, vol.107, pp.52-60, 2019.
[27] M. Zhuang, L. Tan, K. Li et al., Fixed-time formation control for spacecraft with prescribed performance guarantee under input saturation, *Aerospace Science and Technology*, vol.119, 107176, 2021.